

# Measurement of excited-state transitions in cold calcium atoms by direct femtosecond frequency-comb spectroscopy

J.E. Stalnaker,<sup>1</sup> Y. Le Coq,<sup>1</sup> T.M. Fortier,<sup>2</sup> S.A. Diddams,<sup>1</sup> C.W. Oates,<sup>1</sup> and L. Hollberg<sup>1</sup>

<sup>1</sup>*National Institute of Standards and Technology,*

*Time and Frequency Division, MS 847 Boulder, CO 80305*

<sup>2</sup>*Los Alamos National Laboratory, P-23 Physics Division MS H803, Los Alamos, NM 87545*

(Dated: October 9, 2018)

We apply direct frequency-comb spectroscopy, in combination with precision cw spectroscopy, to measure the  $4s4p\ ^3P_1 \rightarrow 4s5s\ ^3S_1$  transition frequency in cold calcium atoms. A 657 nm ultra-stable cw laser was used to excite atoms on the narrow ( $\gamma \sim 400$  Hz)  $4s^2\ ^1S_0 \rightarrow 4s4p\ ^3P_1$  clock transition, and the direct output of the frequency comb was used to excite those atoms from the  $4s4p\ ^3P_1$  state to the  $4s5s\ ^3S_1$  state. The resonance of this second stage was detected by observing a decrease in population of the ground state as a result of atoms being optically pumped to the metastable  $4s4p\ ^3P_{0,2}$  states. The  $4s4p\ ^3P_1 \rightarrow 4s5s\ ^3S_1$  transition frequency is measured to be  $\nu = 489\,544\,285\,713(56)$  kHz; which is an improvement by almost four orders of magnitude over the previously measured value. In addition, we demonstrate spectroscopy on magnetically trapped atoms in the  $4s4p\ ^3P_2$  state.

PACS numbers: 42.62.Eh, 39.30.+w, 06.30.Ft

By providing a clockwork to divide optical frequencies down to countable rf frequencies, stabilized femtosecond frequency combs have made possible absolute frequency metrology of cw lasers used to probe atomic transitions at unprecedented levels of accuracy [1, 2, 3, 4, 5]. In addition, direct frequency-comb spectroscopy has been performed in a variety of systems including two-photon and single photon transitions [6, 7, 8, 9]. Here we extend the techniques developed using direct frequency comb spectroscopy to the study of transitions between excited states by performing step-wise spectroscopy in combination with a cw laser. Significantly, we exploit the frequency comb's wavelength versatility to directly excite transitions between excited states of cold calcium (Ca) atoms at 612 nm and 616 nm, eliminating the need for lasers operating at these wavelengths. By utilizing these techniques in conjunction with cold atoms we are able to surmount the low power limitations and have achieved an uncertainty of 56 kHz, despite having only  $\approx 75$  nW of power in the resonant mode.

The frequency comb is generated by an octave-spanning femtosecond mode-locked laser based on Ti:sapphire with a repetition rate of  $\approx 1$  GHz and is described in detail in Ref. [10]. The frequency comb provides  $\approx 10^5$  optical modes that are related to two rf frequencies by

$$\nu_n = f_0 + n f_{\text{Rep}}, \quad (1)$$

where  $n$  is the mode number,  $f_0$  is the carrier-envelope offset frequency and  $f_{\text{Rep}}$  is the repetition rate of the laser. The carrier-envelope offset frequency is stabilized by use of the self-referencing method with a  $f$ -to- $2f$  interferometer [11]. The repetition rate is phase locked to a synthesizer referenced to a hydrogen maser. The stabilization of the comb in this manner results in the stabilization of all of the optical frequencies of the comb with fractional uncertainties below the  $10^{-12}$  level in one

second.

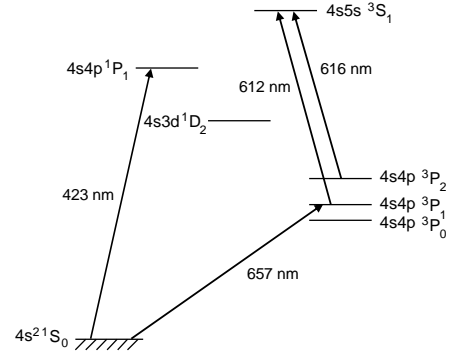


FIG. 1: Low-lying energy levels of Ca.

The comb provides  $\approx 200$  nW of power per optical mode at 612 nm. Because light in the wings of the optical spectrum results from continuum generation within the Ti:S laser crystal the resulting spatial mode is not Gaussian [10]. Consequent difficulties in coupling this light into single mode fiber led us to produce 612 nm light via broadening in highly nonlinear fiber that produced a comparable level of light at 612 nm but with a clean Gaussian mode. The light was then filtered using a 612 nm bandpass interference filter with a passband of 3 nm and sent through  $\sim 20$  m of optical fiber to the Ca atoms. Due to losses in the fiber coupling and in the optics used to deliver the light to the atoms, approximately  $70\ \mu\text{W}$  of light over a 3 nm bandwidth was delivered to the atoms. Using an optical spectrum analyzer we estimate there was approximately 75 nW per optical mode at the resonant wavelength.

An overview of the experiment is shown in Fig. 2. The experiment utilized an apparatus built for an optical frequency standard based on the  $4s^2\ ^1S_0 \rightarrow 4s4p\ ^3P_1\ M = 0$  clock transition in  $^{40}\text{Ca}$  that is described in detail in

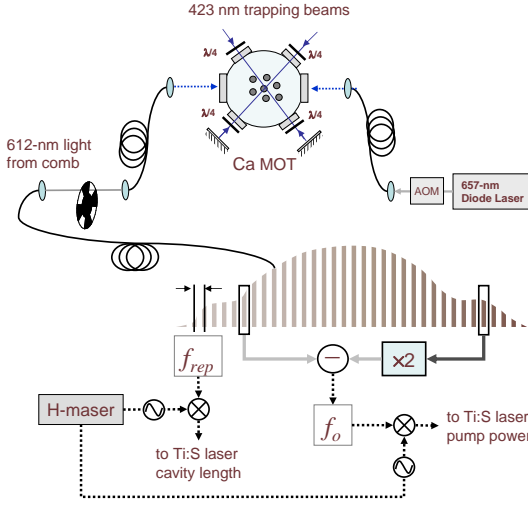


FIG. 2: Schematic of experimental setup for measurement of  $^3P_1 \rightarrow ^3S_1$  transition.

Ref.[12]. The atoms were laser cooled and trapped on the  $4s^2\ ^1S_0 \rightarrow 4s4p\ ^1P_1$  transition at 423 nm (Fig. 1) for 2.5 ms. The resulting sample consisted of  $\approx 6 \times 10^7$  atoms at a temperature of 2 mK. The cold ground-state atoms were excited on the  $4s^2\ ^1S_0 \rightarrow 4s4p\ ^3P_1\ M=0$  transition, which has a natural linewidth of 374 Hz [13], using linearly polarized resonant light at 657 nm consisting of a  $\pi$  pulse with a duration of  $2.5\ \mu\text{s}$ . This excitation selects atoms near zero velocity. Approximately 15 % of the atoms were excited to the  $^3P_1$  state. After a delay of  $40\ \mu\text{s}$  the number of atoms in the ground state was probed with a  $50\ \mu\text{s}$  pulse of 423 nm light resonant with the  $4s^2\ ^1S_0 \rightarrow 4s4p\ ^1P_1$  transition, and the subsequent fluorescence was detected with a photomultiplier tube. The entire cooling-trapping-excitation-probe cycle was repeated every 2.6 ms.

The repetition rate of the frequency comb was scanned over a range of 250 Hz, corresponding to a change of 125 MHz in the optical frequency of the mode used to excite the  $^3P_1 \rightarrow ^3S_1$  transition. When the comb light is resonant with the transition, atoms are excited to the  $^3S_1$  state, from which they decay to the  $^3P_J$  states with an approximate branching ratio of 5 : 3 : 1 for the  $J = 2, 1, 0$  states, respectively. Consequently, roughly 2/3 of the atoms decay to the long lived metastable  $^3P_0$  and  $^3P_2$  states. The decay to these states provides a loss mechanism for the trapped atom number. While atoms in the  $^3P_1$  state can decay back to the ground state and be recaptured in the next loading sequence, the atoms that decay to the metastable  $J = 0, 2$  states do not decay to the ground state. In steady state, this leads to a decrease in the number of atoms detected with the probe pulse. The 612 nm light from the comb was modulated with an optical chopper wheel operating with a 50 % duty cycle at a frequency of 10 Hz. The modulation frequency was chosen to be slow enough so that the 612 nm light leak mechanism would yield a sufficient depletion of the

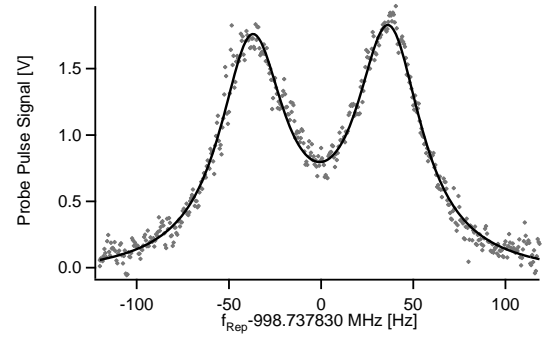


FIG. 3: Typical fluorescence signal as the repetition rate of the laser is scanned over the resonance. The two peaks correspond to transitions to the  $M = \pm 1$  states of the  $^3S_1$  state. The y-axis is the output of the lock-in amplifier; a change of +1 V corresponds to a decrease in the population of the ground state of  $\approx 0.1\%$ . The scan time was  $\approx 20$  minutes.

number of atoms, while still providing sufficient suppression of low-frequency noise. The population transfer was then measured by looking for changes in the probe fluorescence via lock-in detection.

A typical signal is shown in Fig. 3. The two peaks correspond to the  $M_J = \pm 1$  components of the  $4s5s\ ^3S_1$  state, which are split due to the residual field of the magneto-optical trap. The  $M_J = 0$  component is not excited because of the selection rule forbidding  $M_J = 0 \rightarrow M_{J'} = 0$  transitions for states where  $J' = J$ . The 612 nm light is roughly linearly polarized perpendicular to the 657 nm light. We attribute the difference in amplitudes of the two peaks to imperfect polarization of the 612 nm light.

The data were fit to two Voigt profiles with the same widths. This lineshape was empirically seen to correctly describe the data. The actual lineshape is complicated by broadening due to the magnetic field gradient in the center of the trap. The average between the center positions of the two peaks was used to extract the value of the field-free resonance frequency.

In order to determine the optical frequency, the optical mode number of the frequency comb resonant with the transition must be known. This can be accomplished by varying the mode number,  $n$ , by a known amount  $\Delta n$  such that

$$\frac{\delta f_{\text{Rep}}}{f_{\text{Rep}}} \ll \frac{\Delta n}{n^2}, \quad (2)$$

where  $\frac{\delta f_{\text{Rep}}}{f_{\text{Rep}}}$  is the fractional uncertainty in the repetition rate of the resonance as determined from the fit. We identified the optical mode number by adjusting the repetition rate of the comb so as to shift the resonant mode number by exactly 200 modes, corresponding to a change in the repetition rate of the laser of  $\approx 2$  MHz. Data were taken at four different optical modes spanning 200 modes. Based on the consistency of the data we were able to unambiguously identify the mode numbers.

The extracted central frequencies of 15 data sets are shown in Fig. 4. Each data set is the average of two scans of the repetition rate over the resonance; one with increasing frequency and one with decreasing frequency. A difference between the scans taken with increasing frequency and those taken with decreasing frequency was observed. The average difference was 40(26) kHz. We attribute this difference to slow changes in the alignment of the microstructure fiber, leading to changes in the optical power as the laser was scanned over the resonance. As the power changes during the scan, there is an effective shift in the center position of the resonances. The amplitudes of the four peaks (two Zeeman states for both the increasing and decreasing frequency scans) can be used to determine the linear and quadratic drift in the power. This was done for a data set exhibiting a large change in the power during the course of the scan. The coefficients thus determined were used to ascertain the effect of the power changes on the measurement of the peak centers. A shift of 100 kHz was observed as a result of the power drift. However, the effect of the drift canceled in the average of the increasing frequency and decreasing frequency scans at a level of 15 kHz. We therefore assign an uncertainty of 15 kHz due to power variations in the 612 nm light in the extracted frequency.

There is also a systematic uncertainty resulting from the frequency of the 657 nm cw light. The 657 nm light was stabilized to a highly stable optical cavity that has a drift rate of  $\approx 5$  Hz/s, corresponding to a drift of  $\approx 2$  kHz over the course of the scan. This drift results in a drift of the central velocity of the atoms excited by the 657 nm light and therefore a drift in the Doppler effect of the 612 nm transition. The result of the linear drift on the extraction of the transition frequency is much less than that due to the power fluctuations described above and is further suppressed by the combination of the spectra taken with increasing and decreasing repetition rates. Prior to a scan of the 612 nm light, the central frequency of 657 nm light was centered on the zero-velocity class by use of Doppler-free spectroscopy to within  $\approx 50$  kHz. Because the center frequency of the 657 nm light was recentered before each scan, we expect random variations in this error. We increased the statistical errors determined from the fits by 50 kHz to account for this additional effect. After including this effect, the spread of the data remains larger than the uncertainties on the individual scans. We attribute this to a possible motion of the trap during the scan, leading to shifts in the average magnetic field to which the atoms are exposed. We inflate the errors by a factor of 2.7 to get an appropriate chi squared and take this scatter into account. This gives an error on the mean of 54 kHz.

We also considered the effect of ac Stark shifts due to the trapping light. Since the transition of interest is between two excited states, the trapping light is far off resonance with both states. Considering the possible states that could couple to the  $4s4p\ ^3P_1$  state via a 423 nm photon, we estimate the ac Stark shift of this state to

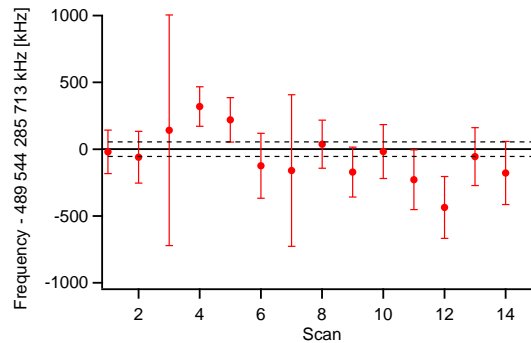


FIG. 4: Measured resonance frequencies for the  $^3P_1 \rightarrow ^3S_1$  transition for 15 different scans. The dashed lines represent the error on the mean.

TABLE I: Errors and the resulting uncertainty in the value of the  $^3P_1 \rightarrow ^3S_1$  transition. The type A uncertainty include effects that average randomly, including the error due to starting frequency of the 657 nm light, the statistical errors as determined from the fits, and the additional scatter, which we attribute to motion of the trap.

Effect	Uncertainty [kHz]
Type A Uncertainty	54
Power changes in the 612-nm light	15
ac-Stark shifts from trapping light	< 0.02
Second-order Zeeman	< 0.010
Frequency Calibration of Comb	< 0.15
Combined Uncertainty	56

be less than 20 Hz. A 423 nm photon brings the  $4s5s\ ^3S_1$  state above the ionization limit, and the ac Stark shift for the state is consequently negligible. The small optical power per mode and the 1 GHz separation of the optical modes make ac Stark shifts from the non-resonant comb modes negligible. Other systematic uncertainties that were considered are presented in Table I.

We arrive at a final value for the transition frequency of

$$\nu(^3P_1 \rightarrow ^3S_1) = 489\,544\,285\,713(56) \text{ kHz.} \quad (3)$$

This value is an improvement by almost four orders of magnitude over the previously measured value as tabulated in Ref. [14]:  $\nu(^3P_1 \rightarrow ^3S_1) = 489544032(450)$  MHz.

In addition to the measurement of the  $^3P_1 \rightarrow ^3S_1$  transition, we were able to observe the  $4s4p\ ^3P_2 \rightarrow 4s5s\ ^3S_1$  transition at 616 nm. This experiment was performed without directly exciting atoms to the  $4s4p\ ^3P_2$  state. Instead, the atoms were populated to the  $^3P_2$  state during the cooling and trapping process. Atoms excited to the  $^1P_1$  state have a  $\approx 10^{-5}$  probability to decay to the  $4s3d\ ^1D_2$  state. These atoms decay predominantly to the  $^3P$  states. Atoms that decay to the  $^3P_2$  state can be magnetically trapped in the magnetic field gradient due

to the MOT trapping coils. By exciting these atoms on the  $4s4p\ ^3P_2 \rightarrow 4s5s\ ^3S_1$  transition at 616 nm we were able to create a repumping mechanism that increases the number of atoms in the ground state, as some of the atoms decay from the  $^3S_1$  state to the  $^3P_1$  state and then back to the ground state. The experiment is identical to that used for the measurement of the  $^3P_1 \rightarrow ^3S_1$  transition frequency, except that there is no 657 nm  $\pi$  pulse needed. The probe signal as the repetition rate of the comb is scanned across the resonance is shown in Fig. 5.

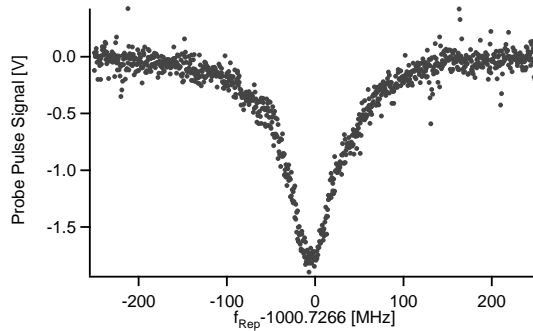


FIG. 5: Fluorescence signal from the 423 nm probe as the repetition rate of the frequency comb is scanned over the  $4s4p\ ^3P_2 \rightarrow 4s5s\ ^3S_1$  transition. A decrease in the voltage corresponds to an increase in the ground-state population.

Only states with  $M = +1$  or  $M = +2$  are magnetically trapped. There are three possible transitions from these states to the  $M = 0$  and  $M = +1$  Zeeman sub-levels of the  $^3S_1$  state. Because of the broadening due to the spatial distribution of the atoms in the magnetic-field gradient, we were unable to resolve these transitions. Consequently, we are unable to determine the Zeeman shift of the transition and cannot calibrate the spatial distribution of the atoms within the magnetic field gradient. While the atoms are distributed over a large volume within the magnetic trap, the 616 nm laser beam intersects only a small region, about 1 mm diameter, of the trap, which is overlapped with the MOT. In order to estimate the magnetic field over the region of the probe beam, we use the measurement of the Zeeman splitting

observed on the 612 nm transition described above, which gives a residual field of  $6.3(3) \times 10^{-4}$  T. We estimate the magnetic field gradient to be  $60(12) \times 10^{-4}$  T/cm in the strong direction. Using these values, and assuming a Gaussian spatial and velocity distribution of atoms over the magnetic field region, gives an estimate for the shift of the different transitions. We find the transition frequencies shift by  $-13$  MHz,  $-9$  MHz, and  $4$  MHz for the  $M = 1 \rightarrow M = 0$ ,  $M = 2 \rightarrow M = 1$ , and  $M = 1 \rightarrow M = 1$  transitions, respectively. If equal weights for the three transitions are assumed and the different broadening of the transitions is included, the effective shift of the resonance is  $-4$  MHz. Due to uncertainties in the relative excitation rates for the different transitions, along with uncertainties in the alignment of polarization with respect to the magnetic field gradients, we assign a 9 MHz uncertainty, along with a +4 MHz correction, to the measured frequency. Given this large uncertainty, we arrive at a value of

$$\nu(^3P_2 \rightarrow ^3S_1) = 486\,370\,098(9) \text{ MHz.} \quad (4)$$

This value is an improvement by a factor of 50 over the current value listed in Ref. [14] of  $\nu(^3P_2 \rightarrow ^3S_1) = 486\,369\,853(450)$  MHz.

We have performed a measurement of the  $4s4p\ ^3P_1 \rightarrow 4s5s\ ^3S_1$  transition in calcium using the direct output of a femtosecond frequency comb. This experiment demonstrates the versatility of direct frequency-comb spectroscopy by combining it with precision cw laser spectroscopy to achieve high-precision absolute frequency measurements of transitions between excited states at wavelengths that are otherwise difficult to produce.

We thank J. Torgerson and Los Alamos National Laboratory (LANL) for supporting the development of the 1 GHz Ti:Sapphire laser. Additional funding came from the National Institute of Standards and Technology. T.M. Fortier and J.E. Stalnaker acknowledge the support of Director's funding from LANL and the National Research Council, respectively. This work was performed by NIST and is not subject to U.S. copyright

- 
- [1] W.H. Oskay, *et al.*, Phys. Rev. Lett. **97**, 020801 (2006).
  - [2] A.D. Ludlow, M.M. Boyd, T. Zelevinsky, S.M. Foreman, S. Blatt, M. Notcutt, T. Ido, and J. Ye, Phys. Rev. Lett. **96**, 033003 (2006).
  - [3] H.S. Margolis, G.P. Barwood, G. Huang, H.A. Klein, S.N. Lea, K. Szymaniec, and P. Gill, Science **306**, 1355 (2004).
  - [4] E. Peik, B. Lipphardt, H. Schnatz, T. Schneider, Chr. Tamm, S.G. Karshenboim, Phys. Rev. Lett. **93**, 170801 (2004).
  - [5] M. Fischer, *et al.*, Phys. Rev. Lett. **92**, 230802 (2004).
  - [6] A. Marian, M.C. Stowe, D. Felinto, and J. Ye, Phys. Rev. Lett. **95**, 023001 (2005).
  - [7] V. Gerginov, C.E. Tanner, S.A. Diddams, A. Bartels, and L. Hollberg, Opt. Lett. **30**, 1734 (2005).
  - [8] S. Witte, R.Th. Zinkstok, W. Ubachs, W. Hogervorst, and K.S.E. Eikema, Science **307**, 400 (2005).
  - [9] T.M. Fortier, Y. Le Coq, J.E. Stalnaker, D. Ortega, S. A. Diddams, C.W. Oates, and L. Hollberg, Phys. Rev. Lett. **97**, 163905 (2006).
  - [10] T.M. Fortier, A. Bartels, and S.A. Diddams, Opt. Lett. **31**, 1011 (2006).
  - [11] D.J. Jones, S.A. Diddams, J.K. Ranka, A. Stentz, R.S. Windeler, J.L. Hall, and S.T. Cundiff, Science **288**, 635 (2000).
  - [12] C.W. Oates, F. Bondu, R.W. Fox, and L. Hollberg, Eur.

Phys. J D **7**, 449 (1999).

[13] C. Degenhardt, *et al.*, Phys. Rev. A **72**, 62111 (2005).

[14] J. Sugar and C. Corliss, J. Phys, Chem. Ref. Data **14**,

supplement 2 (1985).